Potential Benefits of Polymers in Soil Erosion Control for Agronomical Plans: A Laboratory Experiment

Tugrul Yakupoglu [1],* [ID]**, Jesús Rodrigo-Comino** [2] [ID] **and Artemi Cerdà** [3] [ID]

[1]   Department of Soil Science & Plant Nutrition, Faculty of Agriculture, Yozgat Bozok University, Campus of Erdogan Akdag, 66900 Yozgat, Turkey

[2]   Instituto de Geomorfología y Suelos, Department of Geography, Málaga University, Campus of Teatinos s/n, 29071 Málaga, Spain; rodrigo-comino@uma.es

[3]   Soil Erosion and Degradation Research Group, Department of Geography, Valencia University, Blasco Ibàñez, 28, 46010 Valencia, Spain; artemio.cerda@uv.es

*   Correspondence: tugrul.yakupoglu@bozok.edu.tr; Tel.: +90-354-242-1028

check for updates

Abstract: New management and techniques to reduce soil and water losses are necessary to achieve goals related to sustainability and develop useful agronomical plans. Among the strategies to reduce soil losses, the use of polymers has been studied but little is known about the effect of them on soil aggregates under extreme rainfall conditions. The main aim of this study was to compare the effects of polyacrylamide (PAM) and polyvinyl alcohol (PVA) on initial soil erosion process activation. We applied both products on soils and soil aggregate stability was measured on polymer treated and control plots. Laboratory erosion plots (pans) were placed on 15% slope, and sequential simulated rainfalls (under dry and wet conditions) with 360 mm h^{-1} intensity were applied for 12 min. Time to runoff, total runoff, runoff sediment yield, and splash sediment yield were determined. The results show that polymers do not delay runoff initiation; however, they reduced total runoff, sediment yield, and soil transported by the splash. PVA was not effective in reducing the total runoff during the first rainfall being PAM more effective in this way. However, under the sequential rainfall, both polymers obtained positive results, showing PAM some improvements in comparison to PVA. The effect of the polymer to reduce soil transported by splash after performing the second rainfall simulation was clearly demonstrated, meanwhile the effects during the first simulation were not significant. The effectiveness of the polymers on soil aggregates increased with increasing aggregate size. The application of polymers reached the highest efficiency on aggregates of 6.4 mm in diameter.

Keywords: soil aggregate; polyacrylamide; polyvinyl alcohol; erosion; agricultural soil management

1. Introduction

Global change affects biogeochemical cycles, and soils play a key role in these cycles [1,2]. Soil erosion is a threat to soil sustainability and scientific research is looking for new solutions to reduce and control the accelerated soil erosion rates in agricultural lands [3,4]. Soil erosion is a worldwide problem that needs solutions to achieve sustainable production of fibers and food for humankind and to maintain geochemical, hydrological, and erosional cycles in a stable condition [5,6]. Soils play a key role to achieve the sustainable development goals (SDG) that the United Nations defined [7].

Research on soil erosion has been focused on basins, catchments, and hillslope scales [8,9]. However, it is also vital to understand soil erosion processes at the pedon and aggregate scales to find specific remediation strategies and achieve sustainable management of the soil system. Within this objective, it is relevant to determine the driving factors of soil erosion [10]. At the pedon scale, factors

such as organic carbon [11,12], porosity [13], soil texture [14,15], bulk density [16], and aggregate stability [17] have been found to be factors in controlling soil erosion.

Aggregate stability is an important soil property that determines the cohesion between soil particles, but there is a lack of information about which control measures can effectively improve cohesion in agricultural fields [18,19]. It is known that a cover of vegetation or litter will improve the stability of the aggregates [20], and this will protect the ecosystem service provided by soil since soil erosion will be also reduced [21]. However, many farmers are resistant to adopt straw or mulch cover [22,23]. Thus, it is necessary to find solutions to mitigate the acceleration of soil erosion rates in agricultural lands and enhance infiltration [24] that will be well-accepted by the farmers. For this reason, integrated studies in which soil conservation practices are based on rainfall erosivity are meaningful.

Recent studies about soil erosion control measures paid attention to the use of mulches [25], cover crops [26], or geotextiles [27,28] as they reduce the rainfall erosivity and improve soil conditions which result in a lower soil erodibility. Another set of strategies is based on the management: plant species and grazing pressure in rangelands [29], land abandonment [30] or land preparation and vegetation covers [31].

In this way, polymers have been also reported as useful tools to reduce soil erosion rates and increase soil fertility [32,33]. Specifically, polyacrylamide (PAM) and polyvinyl alcohol (PVA) have been used in erosion studies since the 1950s [34]. It is emphasized as a general result that even when the polymers are applied to the soil surface at low doses, they may have significant positive effects on the improvement of aggregates and structural stability [35,36]. It was reported that flocculent materials reduce the adverse effects of disruptive and destructive forces by increasing binding forces among granules [37]. Several decades ago, Vleeschauwer et al. [38] studied the effect of PAM on soil physical properties, determining that its application was able to increase porosity and water infiltration rates into the soil profile, positively affecting aggregate stability. Chiellini et al. [39] examined the adsorption of PVA by montmorillonite, quartz sand, and farm soil. Their findings demonstrated that PVA adsorption is increased when montmorillonite content increases, whereas quartz sand did not absorb PVA. They also demonstrated that PVA adsorbed on montmorillonite exhibits a much slower mineralization rate than the non-absorbed PVA remaining in solution. Slower mineralization rates of absorbed PVA inhibit its biodegradation.

These potential benefits of polymer application are significantly affected by their complex properties (molecular weight, load type, and charge density) and soil properties (texture, organic matter content, clay mineralogy, soil solution composition, and concentration) [40–42]. One of the soil properties affecting polymer activity is the aggregate size. The aggregate size group dominating an environment can vary according to slope positions. Kussainova et al. [43] observed that soil aggregates larger than 60.3 mm dominate on footslopes, and that aggregates smaller than 2 mm are predominant in summits and backslopes. However, in agricultural fields, tillage can affect soil aggregate sizes and, subsequently, bulk density can vary along the hillslope [44]. Therefore, erosion sensitivity based on soil structural stability also varies in time and according to land cover and management [45,46]. Aggregate formation in these agricultural ecosystems drastically changes over the seasons, and the average resistance duration of the macro-aggregates can be around 27 days, with a minimum resistance of 5 days [47].

In order to obtain the most effective result from polymer application, the most appropriate polymer type, application form, and dosage must be determined for each soil. To reduce soil erosion, the effectiveness of each polymer applied on the soil will be closely related to the dynamics of aggregates disintegration, which is highly influenced by rainfall erosivity as it was demonstrated by other authors in non-cultivated soils [48].

The main aim of this study was to investigate the effects of PAM and PAV applied to soil aggregates with different sizes on soil detachment to understand the initial soil erosion mechanisms.

The experiments were carried out under indoor simulated rainfall experiments to achieve the highest accuracy under controlled laboratory conditions.

2. Materials and Methods

2.1. Study Area

This study was carried out using soil samples taken from an area located within the borders of Kahramanmaras Sutcu Imam University Avsar Campus (Figure 1a; Kahramanmaras Province, Turkey, 4162434 N; 606322 E). The study site is located in an area characterized by a Mediterranean climate with a mean total annual rainfall of 710 mm, with the most rain concentrated from winter to the first weeks of spring. The summers are hot and dry. The mean annual temperature is 16.5 °C, with the highest monthly average temperature in July and the lowest average one in January. The soil moisture regime is Xeric and, the temperature regime Mesic [49] as stated by the Turkish Republic General Directorate of Meteorology [50]. Average slope inclinations are 15%. Quaternary deposits are the more predominant and they are composed of Pliocene materials that come from the slope as debris, skirt rashes, and young alluviums, and middle Miocene with conglomerates, pebbles, sand and clay materials stratified by the alternation of layers about 2–3 m thick. The stratigraphic layers of the Pliocene have been tilted 15–30° north-west from neotectonic forces.
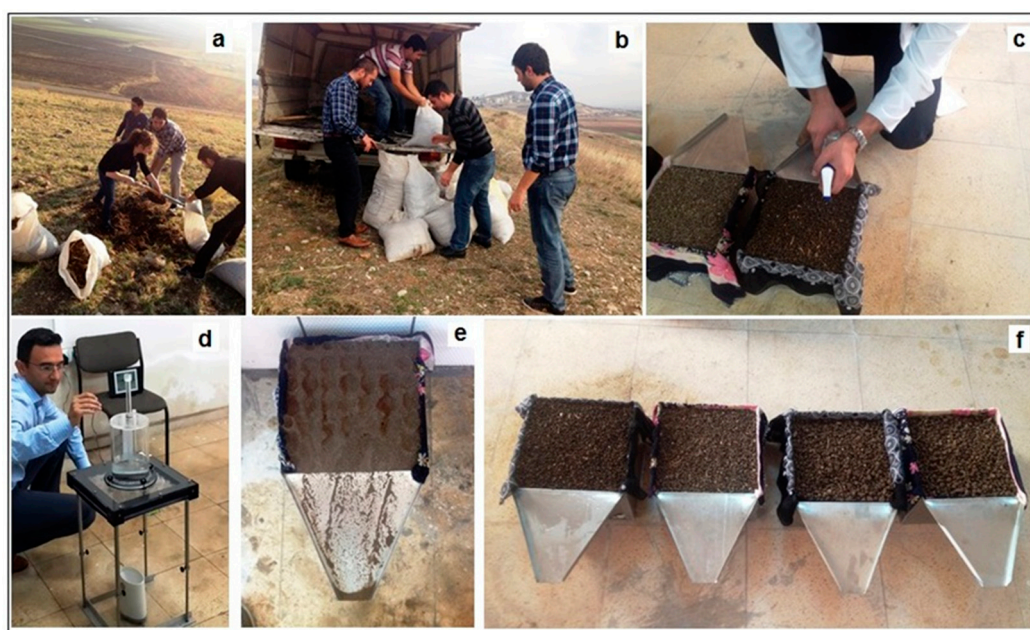

Figure 1. Soil sampling procedure and rainfall simulations under laboratory conditions. (**a**) Study area; (**b**) soil sampling; (**c**) polymer spraying; (**d**) mini-rainfall simulator; (**e**,**f**) rainfall simulation plots.

2.2. Soil Characteristics and Erodibility

Soil profile characteristics and soil properties are presented in Table 1. Five different soil horizons can be distinguished. Disturbed soil samples were taken from the most superficial soil horizon (Figure 1b; 0–25 cm). The superficial horizon is an Ap, the main color is 7.5YR4/3, and soil texture is characterized as 376 g kg^{-1} sand, 231 g kg^{-1} silt and 393 g kg^{-1} clay. The pH value is 8.3, total CaCO$_3$ is 117 g kg^{-1} and soil organic carbon is low ($\approx$20 g kg^{-1}). Thus, soils can be classified as Typic Xerochrepts [49]. Wet aggregate stability reaches 41% and dispersion ratio 16.5%. The structural analysis showed results of about 52.1. The mean weight diameter was 2.1 mm. Finally, the K factor of RUSLE was calculated to show the relationship between organic matter content, particle size distribution, structural status, and hydraulic conductivity of the soil [51]. There were no high contents

of stones in the soil profile, therefore, no corrections were made on the K factor. Final results registered mean values of 0.1 Mg ha h ha^{-1} MJ^{-1} mm^{-1}.

Table 1. Soil profile characteristics and some properties.

Horizon	Depth (cm)	Color (dry; wet)	Sand (g kg^{-1})	Silt (g kg^{-1})	Clay (g kg^{-1})	pH	Salinity (%)	CEC (meq 100 g^{-1})	Total CaCO$_3$ (g kg^{-1})	SOM (g kg^{-1})
Ap	0–25	7.5YR4/3; 7.5YR4/3	376	231	393	8.3	0.05	38.0	117	207
AC	25–45	7.5YR6/4; 7.5YR5/4	590	280	130	7.44	0.10	19.13	244	103
1C	45–107	7.5YR8/2; 10YR6/4	723	197	80	7.84	0.06	11.13	285	038
2Ck1	107–150	7.5YR8/2; 7.5YR7/4	153	583	264	7.55	0.10	22.52	661	026
2Ck2	+150	7.5YR8/2; 10YR7/4	275	459	266	7.35	0.05	22.17	454	006

CEC: Cation-exchange capacity; Total CaCO$_3$: Calcium carbonate; SOM: Total soil organic matter content.

2.3. Polymer Application

For this reason, two types of polymers with different molecular weights and bond types were used in this study. Soil aggregates with different sizes (<1, 1–2, 2–4, 4–6.4, >6.4 mm, and all aggregates mixed and named 'All') were selected by means of sieving. The initial moisture content of air-dried aggregates was 12 ± 1% basis on the dry weight. The two polymers were: (i) a polyacrylamide (PAM) with a molecular weight of 0.2 Mg mol^{-1} and a charge density of about 20%; and, (ii) polyvinyl alcohol (PVA) with a molecular weight of 0.07 Mg mol^{-1} and a charge density of about 18%. These polymeric materials have an anionic character. PAM ((-CH$_2$CHCONH$_2$-)$_n$) is a linearly-linked, water-soluble acrylamide sodium acrylate copolymer and PVA ((-CH$_2$OHOH-)$_n$) is a cross-linked vinyl alcohol-acrylic acid which is hydrophilic to a certain solvent temperature. Both conditioners are granular and white in color when dry. These kinds of PAM and PVA are widely used in agricultural practices to enhance soil aggregates stability, but soil erosion studies with these materials are scarce. Both polymers were applied as solutions on air dry aggregates with 6.25 kg ha^{-1} dose (Figure 1c).

2.4. Rainfall Simulation Experiments and Procedures

Rainfall simulation experiments were conducted on laboratory erosion plots (pans: 25 × 25 × 15 cm of width, length, and depth, respectively) by using a mini-rainfall simulator (Figure 1d; Product Code: M1.09.06.E, type LUW, Eijkelkamp Agrisearch Equipment, which was mass-produced by Eijkelkamp firm (Eijkelkamp Soil & Water, Giesbeek, The Netherlands). The mini-rainfall simulator consists of a watering unit with 49 drop formers and a 2300 mL capacity water load unit, which is achieved basically by a Mariotte scheme that regulates the pressure in its reservoir. The drop-forming caps have a length of 10 ± 1 mm and an inner diameter of 0.6 ± 0.08 mm. Sprinkling is effective on a plot of 0.0625 m^2 (Figure 1e). The drop distance of the droppers is 0.4 m.

We applied 360 mm h^{-1} rainfall intensities to test the resistance of soil aggregates. According to this rainfall intensity, the mass of one droplet is 0.106 g and its diameter is 5.9 mm, while the kinetic energy is 4 J m^{-2} mm^{-1} [52]. Calibration attempted to achieve a flow density of 375 mL min^{-1} to produce excellent flow conditions. For this purpose, the height of the glass pipe in the water load reservoir proposed by the manufacturer is calculated using Equation (1) [52] and the height of this pipe is set in the simulator as

$$h = 100 - 0.65t \qquad (1)$$

where *h* (mm) is the height of the pipe between the reservoir and the upper side of the aeration pipe at the beginning of the calibration to achieve the optimum *h* value for raining 375 mL min^{-1}; the value 100 (mm) is the starting position of the aeration tube, 0.65 is a correction factor for temperature (a temperature change of 1 °C causes a flow change of approximately 4 mL min^{-1}); and, *t* is the temperature of the rainfall water in °C.

The intensity measurements of produced simulated rainfall were made using TFA 35.1075 Nexus wireless type mini meteorological station. The uniformity coefficient (CV) was 0.96 calculated by using Equation (2) [53].

$$C_V = [1 - (I_{SD}/I_{mean})] \, 100 \tag{2}$$

where C_V is the Christiansen uniformity coefficient in %; I_{mean} is the mean rainfall intensity in mm h^{-1}, and I_{SD} is the standard deviation of intensity measurements.

Twenty-four hours after the application of the polymer, soil pans were sloped at 15% and subjected to artificial precipitation with an intensity of 360 mm h^{-1} (Figure 1e,f). The technical report for the rainfall simulator [52] explains that the simulated rainfall can be uniformly rained and the low kinetic energy problem caused by the drop distance of 40 cm is overcome by operating the instrument at high intensity. We consider that the erosion event took place when we observed the first degree of aggregates fragmentation, according to van Dijk et al. [54]. To calculate how much time is needed to conduct the rainfall simulation to generate an energy flow of 50 mm h^{-1}, which corresponds to an intensive natural rainfall, we used Equation (3).

$$E_m = 0.29 \left[1 - 0.72 e^{(-0.05 I_m)} \right] \tag{3}$$

where E_m is the kinetic energy of rainfall per unit (MJ ha^{-1} mm^{-1}) and I_m is the rainfall intensity (mm h^{-1}). The total kinetic energy of the natural rainfall obtained was 2.73 MJ ha^{-1} by applying Equation (4), achieving a depth of 10 mm of rain.

$$\sum E_m = E_m \, h \tag{4}$$

where $\Sigma \, E_m$ is the total kinetic energy of rainfall (MJ ha^{-1}), E_m is the kinetic energy of rainfall per unit (mm h^{-1}), and h the total rainfall (mm).

Thus, it was estimated that the instrument needs about 12 min of sprinkling time to produce a total of 2.73 MJ ha^{-1} energy flows while generating a rain of 360 mm h^{-1} with a rain area with 0.0625 m^2 taken into account. Thus, the duration of rainfall was 12 min for each simulated rainfall application. Distilled water was used in the rainfall operations.

Elapsed time to runoff generation (Tr; seconds), the total amount of runoff (R; mm), sediment yield (Sy; g m^{-2}), and transported soil by splash on both sides of the pan (Sp-Sy) were considered as variables. During the rainfall simulation, water and soil losses were quantified every two minutes. Samples were measured under laboratory conditions by filtering and drying. Two days after the first rainfall simulation experiments on all aggregate sizes, sequential simulated rainfalls were repeated, covering the pans during the waiting time between simulations. Findings obtained from the second sequential rainfall were considered as a second repetition.

2.5. Statistical Analysis

First and second rainfall simulations were thought as different experiments (paired-experiments under different soil moisture conditions). An ANOVA test was applied to the data, which show a normal distribution (Shapiro–Wilk test) for evaluating the effects of applications on the measured variables. After that, a Duncan test was also applied in order to compare the plots in terms of effectiveness among each other. Finally, a dependent sample *t*-test was conducted to compare the data sets obtained in the first and sequential rainfall experiments and observe the dependence among them. All statistical analyses were conducted with SPSS 23.0 computer package [55].

3. Results

Figure 2 shows the time to runoff generation results in a bar graph with the different aggregate sizes. Polymer applications partially delayed runoff generation compared to the control plot. In addition, surface runoff starts earlier under sequential rainfall in all the erosion pans and different soil

aggregate sizes. After the first run, runoff is generated the earliest at 35 s in the pan in which are placed <1 mm aggregates with no polymer application, meanwhile, for the largest aggregate size (>6.4 mm) runoff started the latest at 338 s with PAM.
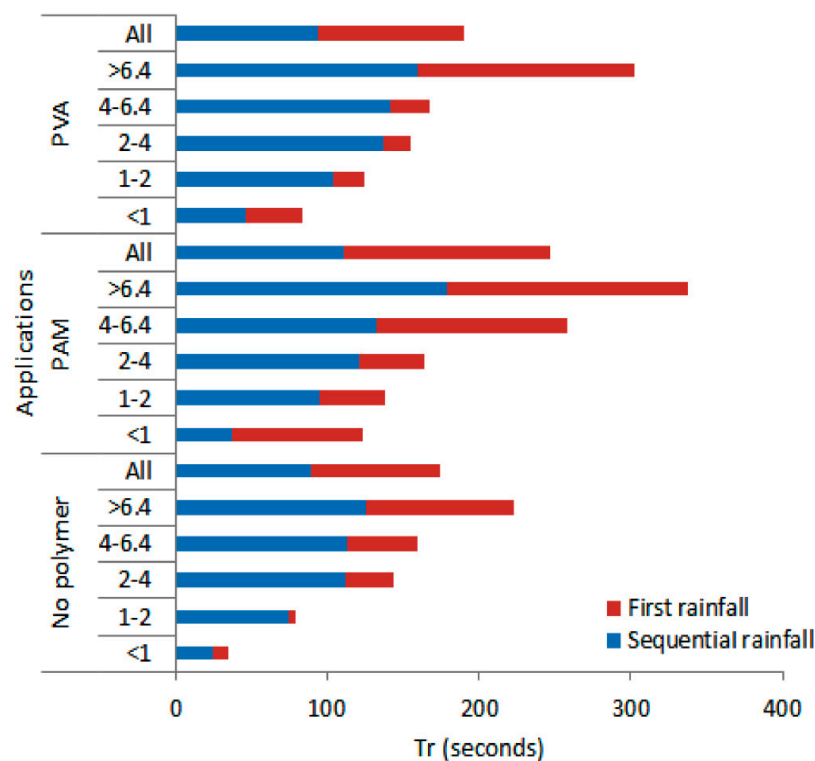

Figure 2. Time to runoff generation results per aggregate sizes. PAM: Polyacrylamide; PVA: Polyvinyl alcohol; Tr: Time to runoff.

In Table 2, total runoff (R), sediment yield (Sy), and sediment yield mobilized by splash (Sp-Sy) results are added. Under first rainfall, the highest R values are measured for soil aggregates smaller than <1 mm in all the experiments. Specifically, PAM shows the highest runoff amount (45.1 mm) and PVA the lowest one (42.4 mm). The highest Sy values vary from 110 (<6.4 mm) to 2926 g m^{-2} (>1 mm) for the control plots, from 86.5 to 2071 g m^{-2} (>1 mm) in PAM and from 53 (>6.4 mm) to 2310 g m^{-2} (>1 mm) in PVA. PVA produces the lowest Sy values (113 g m^{-2}) and the highest one is registered in the control plot (197 g m^{-2}). Sp-Sy shows the highest values again in the control plot (9 g m^{-2}), but the lowest is registered on the PAM plot (4.0 g m^{-2}).

In Table 3, soil erosion results after the sequential simulated rainfall are included. The highest runoff amounts are found for soil aggregates smaller than <1 mm in all the experiments, but differences are lower than in the first run. However, the control plot shows the highest R, reaching 48 mm. In contrast, PAM and PVA show lower values, reaching 37 and 39 mm, respectively. In the control plot, the highest Sy values are registered, and values for all aggregate sizes are two and three magnitudes greater. For both PAM and PVA, sediment yield registers higher values than after the first run, but lower than the control one (160 and 145 mm, respectively). Sp-Sy shows similar values for all the plots (with and without polymer applications). The lowest values are found on the PVA plot (145 mm).

Table 2. Mean values of soil and water losses under the first simulated rainfall.

Application	Initial Aggregate Size (mm)	R (mm)		Sy (g m^{-2})		Sp-Sy (g m^{-2})	
		Mean	SD	Mean	SD	Mean	SD
No polymer	<1	46.4	2.3	2925.6	263.6	18.1	3.3
	1–2	38.8	2.9	332.5	10.4	16.2	2.5
	2–4	32.0	1.4	231.0	80.3	9.8	0.8
	4–6.4	26.2	3.7	143.4	26.9	8.2	0.2
	>6.4	23.6	0.6	110.1	17.2	6.3	2.0
	All	34.1	0.1	196.5	24.3	8.6	1.2
PAM	<1	45.1	2.6	2071.0	35.3	18.0	1.4
	1–2	34.7	2.1	307.6	16.4	3.8	0.8
	2–4	21.5	3.1	131.2	33.5	3.6	0.7
	4–6.4	18.3	2.9	116.2	0.2	2.1	0.1
	>6.4	12.6	0.3	86.5	15.5	2.0	0.8
	All	24.8	2.8	156.5	6.6	4.0	0.3
PVA	<1	42.4	2.7	2310.2	89.1	13.8	1.1
	1–2	34.9	1.6	176.4	37.8	7.9	1.7
	2–4	29.1	5.6	107.5	27.1	7.4	0.7
	4–6.4	21.9	2.3	69.1	16.2	4.0	1.1
	>6.4	14.3	0.1	53.3	2.1	3.2	0.8
	All	34.4	2.0	112.6	7.9	6.4	1.1

PAM: polyacrylamide, PVA: polyvinyl alcohol; R: total runoff, Sy: transported sediment quantity by runoff, Sp-Sys: sediment yield by splash on two sides of erosion pan, SD: Standard deviation.

Table 3. Mean values of soil and water losses under sequential simulated rainfall.

Application	Initial Aggregate Size (mm)	R (mm)		Sy (g m^{-2})		Sp-Sy (g m^{-2})	
		Mean	SD	Mean	SD	Mean	SD
No polymer	<1	61.1	3.5	4699.3	357.2	21.1	6.8
	1–2	48.1	2.5	794.2	19.6	20.3	0.1
	2–4	43.6	2.1	314.5	0.6	12.0	5.7
	4–6.4	37.3	5.2	156.0	19.0	10.7	1.1
	>6.4	32.2	0.3	137.9	6.9	12.3	4.2
	All	47.9	0.2	477.3	68.2	13.2	4.4
PAM	<1	55.0	0.1	2428.0	794.8	19.6	1.8
	1–2	44.6	2.2	330.8	4.0	13.8	3.7
	2–4	28.9	3.1	186.6	61.9	10.3	1.8
	4–6.4	26.5	2.6	126.7	4.9	6.4	5.1
	>6.4	18.7	3.2	89.1	1.3	5.5	0.7
	All	36.9	0.3	160.1	19.9	12.3	2.9
PVA	<1	52.0	0.1	2844.2	751.3	18.7	3.3
	1–2	44.8	6.4	304.8	21.7	12.0	5.7
	2–4	40.5	3.0	138.8	14.3	9.1	0.2
	4–6.4	36.5	1.3	117.0	1.7	6.8	1.6
	>6.4	25.6	2.5	71.8	4.4	6.3	1.7
	All	39.0	1.4	145.3	22.0	11.4	4.1

R: total runoff, Sy: transported sediment quantity by runoff, Sp-Sys: sediment yield by splash on two sides of erosion pan, SD: Standard deviation.

To observe the differences among applications and initial aggregate size groups, an ANOVA test was conducted and results are presented in Table 4. R values are significant for the polymer applications for the first ($p < 0.01$) and sequential rainfall ($p < 0.001$). Initial aggregate size also affects runoff under both runs ($p < 0.001$). Sy values show under both rainfall simulations highly statistical significance ($p < 0.001$). Under first rainfall, the effect of applications on Sy is not statistically significant, but under sequential rainfall statistically significant differences can be found ($p < 0.05$). Sp-Sy under

the first run does not show statistical significance among applications, but it is significant among initial aggregate size groups ($p < 0.05$). In contrast, both results are statistically significant after the second run.

Table 4. ANOVA results of obtained data.

Variables	Rainfalls	Variation Source		
		Applications	Initial Aggregate Size Groups	R^2
R	First rainfall	**	***	0.88
	Sequential rainfall	***	***	0.97
Sy	First rainfall	***	***	0.99
	Sequential rainfall	***	***	0.98
Sp-Sy	First rainfall	ns	**	0.65
	Sequential rainfall	*	***	072

R: total runoff, Sy: transported sediment quantity by runoff, Sp-Sys: sediment yield by splash on two sides of erosion pan, ns: not significant; * Statistical significance at a level of 0.05, ** Statistical significance at a level of 0.01, *** Statistical significance at a level of 0.001.

PAM is the most effective application to reduce R generated under the first rainfall (Table 5). However, the effectiveness of PVA is not different from the control plot. Under sequential rainfall, results follow the order no polymer<PVA<PAM in terms of effectiveness in reducing R, being different from each other statistically. When compared to no polymer applications, the polymers succeed in reducing Sy in comparison to the control plot, but there is no statistical difference between the polymers. Finally, no significant statistical difference is found in Sp-Sy after the first run, but the difference is significant after the second run. Polymers were demonstrated to be successful in reducing Sp-Sy.

Table 5. Duncan test results through the applications ($\alpha = 0.05$).

Variables	Application	Subgroups	Application	Subgroups
		First Rainfall		Sequential Rainfall
R	PAM	26b	PAM	350c
	PVA	29ab	PVA	39b
	No polymer	33a	No polymer	45a
Sy	PVA	471b	PAM	553b
	PAM	478b	PVA	603b
	No polymer	656a	No polymer	1096a
Sp-Sy	PAM	ns	PVA	10b
	PVA	ns	PAM	11b
	No polymer	ns	No polymer	14a

ns: not significant statistically; PAM: polyacrylamide, PVA: polyvinyl alcohol; R: total runoff, Sy: transported sediment quantity by runoff, Sp-Sys: sediment yield by splash on two sides of erosion pan.

Under the first run, the most effective initial aggregate sizes where polymers reduced R was from 4–6.4 to >6.4 mm sizes, which are statistically similar, meanwhile, the least effective polymer application was for aggregates <1 mm (Table 5). There is statistically no difference between Rs from pans of mixed aggregates (all) and from 1 to 2 mm size. Under sequential rainfall, all of initial aggregate size groups show statistical differences from each other in terms of their effects on R. After conducting the first rainfall, Sy from 2 to >6.4 mm showed a statistical relationship. The other sizes (<1 and 1–2 mm) register differences from each other and from the other ones. After the sequential rainfall, similar results are found. Under the first rainfall, the effects of polymers on all initial aggregate size groups in reducing Sp-Sy are statistically the same except for <1 mm. Under sequential rainfall, the most ineffective groups for reducing Sp-Sy are <1 mm and 1–2 mm, with no statistical difference among them (Table 6).

Table 6. Duncan test results through the initial aggregate sizes ($\alpha = 0.05$).

Variables	Initial Aggregate Size (mm)	Subgroups	Initial Aggregate Size (mm)	Subgroups
		First rainfall		Sequential rainfall
R	>6.4	16e	>6.4	25f
	4–6.4	22de	4–6.4	33e
	2–4	27cd	2–4	37d
	All	31bc	All	41c
	1–2	36b	1–2	45b
	<1	44a	<1	56a
Sy	>6.4	83c	>6.4	99c
	4–6.4	109c	4–6.4	133bc
	All	155c	2–4	213bc
	2–4	156c	All	260bc
	1–2	272b	1–2	476b
	<1	2435a	<1	3323a
Sp-Sy	>6.4	3.8b	4–6.4	7.9c
	4–6.4	4.7b	>6.4	8.0c
	All	6.3b	2–4	10.4bc
	2–4	6.9b	All	12.3bc
	1–2	9.3b	1–2	15.3ab
	<1	16.6a	<1	19.8a

R: total runoff, Sy: transported sediment quantity by runoff, Sp-Sys: sediment yield by splash on two sides of erosion pan.

Finally, a comparison of two runs by dependent sample *t*-test in terms of R, Sy, and Sp-Sy are added in Table 7. All three variables are affected by successive rainfall simulations at different statistical levels. In general, the highest soil and water losses occur after the second simulated rainfall.

Table 7. Comparison of first and sequential rainfalls with the dependent sample *t*-test for Tr, Sy, and Sp-Sy.

Pairs	Paired Differences					*t*	df	Sig. (2-Tailed)
	Mean	Std. Deviation	Std. Error Mean	95% Confidence Interval of the Difference				
				Lower	Upper			
First sequential rainfall (R)	−10	4	0.7	−11	−8	−13	35	0.000
First sequential rainfall (Sy)	−215	465	77	−373	−58	−2.7	35	0.009
First sequential rainfall (Sp-Sy)	−4	6	1	−6	−2	−4.3	35	0.000

R: runoff; Sy: transported sediment quantity by runoff, Sp-Sys: sediment yield by splash on two sides of erosion pan, ns: not significant statistically.

4. Discussion

The use of small portable rainfall simulators is considered as a valuable technique to estimate initial soil and water losses and is highly used to assess the effectiveness of soil erosion control measures. However, the use of mini-rainfall simulators is not common in the scientific literature. Small plots (<1 m^2) have been the subject of criticism by several authors [56,57] related to the representativeness of these results to larger scales of plot size and rainfall intensity. It was decided to work with this simulator since it is standardized and hydrometeorological characteristics have been well-specified and defined by the company. Therefore, it can be used to easily obtain results that can be compared to results from future research, and the measurements and experiments can be repeated during other

seasons and under field conditions. The rainfall intensity generated by the mini-rainfall simulator is influenced by the viscosity of the sprinkler water used and by the clogging of the capillary sprinkler heads. For this reason, the simulator was calibrated prior to using it. It has been confirmed that specific factors, soil properties, and solutions can be detected and quantified only at the pedon scale.

Through our experiments, we were able to confirm that the mini-rainfall simulator is useful to evaluate different soil erosion control measures (polymers). Therefore, this study can be included in the body of research that focuses on soil erosion research under laboratory conditions with direct application to field conditions as the accuracy we achieved in the laboratory was the highest [58,59].

Aggregate stability is one of the factors that enhances resistance to soil erosion [19,60] but little is known about how to improve this stability in agricultural soils with different aggregate sizes. We observed in our study that aggregate sizes show different responses to raindrop impact under high rainfall intensities. The dose was selected according to results of preliminary experiments and a literature search of comparable studies [61–64].

Splash effect impact on soil aggregates is not a well-known process, though its relevance is often highlighted in the literature [48,65]. Our results demonstrated that the most resistant soil aggregates are the largest sizes compared to the smallest ones (Table 7). In agricultural fields, the stability of macroaggregates is affected by management practices and mineral soil components added as manure or mulching that change their hydrophilic nature [66–68]. In this context, the use of polymers such as PAM and PVA was demonstrated to be effective in increasing structural stability, decreasing runoff generation, splash, and soil losses. The potential benefits of polymers are influenced significantly by their complex: molecular weight, load type, and charge density [42,69,70].

By using a mini-rainfall simulator on different soil aggregate sizes, we detected that soil aggregation is developed in a hierarchical order. The micro-aggregates are generated and then will be joined into new macroaggregates, acting as building blocks for larger aggregates [71]. However, as for our tested soils, if this aggregation is not possible because of the tillage or extreme rainfall events, soil erosion will take place inevitably. Therefore, the application of polymers will be a determinant factor to improve aggregation [28]. In macroaggregates, where capillary roots and various hyphae play a role as binders, which also act as aggregates. This effect is temporary and these roots and hyphae serve as cores of these micro-aggregates inside the macroaggregates [16]. Due to the temporary binding characteristic of these roots and hyphae, aggregates cannot hold together indefinitely and disintegrate into fragments. These fragments covered with a glue-like material formed during fragmentation are covered by clay particles and a new structure of macroaggregate forms in which a micro-aggregate is involved [72]. Thus, PAM and PVA effects applied to the aggregates with different initial sizes have varied, since the durability of each aggregate size is different.

Small sized (micro-sized) inorganic and organic stabilizer compounds can be integrated into the micro-aggregates, stabilizing them, but bigger roots and hyphae play a part as binders in the stabilization of the macroaggregates. This can be because the stomas in micro-aggregates are micropores and the stomas between micro-aggregates are bigger pores (macropores) [73]. Because the binding agent acts in the soil system according to the stoma size, stoma size distribution largely affects size and stability. Stoma size distribution is an active feature of the soil in aggregation and fragmentation, which is why PAM and PVA activity on structural stability have differed with the change in initial sizes of aggregates in the study.

In the study conducted by Levy and Miller [74], it was discovered that anionic polymers penetrate the stomas more easily and are absorbed in the inner surface since the stomas between big aggregates will be wide. Researchers have noted that the durability of these aggregates would be long as the applied polymers have a chance to penetrate bigger aggregates from both inside and outside. In a study carried out under low-kinetic energy rainfalls [75] under laboratory conditions, soil degradation has been achieved at the same level in different textured soils, although the resistance of soil to shredding is different in distinct textured soils [76,77].

We also conclude that one of the most important key factors that can modify the stability of the soil aggregate as other authors mentioned is the antecedent soil moisture content before conducting the experiments [47,73]. In this study, the activation of the runoff and soil particle yield after the sequential rainfall was higher than after the first rainfall, which, in fact, it could be attributable in that the soil is not completely dry out between two rainfall events. Moreover, some soil aggregates start to be affected and disintegrated. After that, aggregates were most susceptible to the separation prior to performing the sequential rainfall, since the reconnection, which is likely to occur due to drying, did not occur in this period.

In the future, we consider that some future lacks should be also filled in order to improve the knowledge about the impact of polymers on soil the initial soil erosion and their effectivity: (i) increasing the plot size and testing different soils with other soil texture and organic matter contents; (ii) assessing changes of soil erosion resistance after polymer application at short- and medium-terms; (iii) performing an economic analysis of the viability to apply polymers at the larger scales in agricultural fields; and (iv) comparing their effects to other natural control soil erosion measures such as straw, grass cover, or catch crops.

From the point of view of new challenges to be researched to achieve proper management, we suggest using a combination of two strategies to control soil and water losses. This will increase the efficiency of the strategy from an environmental and pure economic point of view. We must research in the future not only polymer impact on runoff and erosion but also how straw—such as Rodrigo-Comino et al., [78] demonstrate—is very efficient in soil erosion control but can be even more in combination with the use of polymers that will reduce soil erodibility. This approach should be also applied to the use of chipped pruned branches, no-tillage, geotextiles, grass strips, etc. and other strategies that with the combination with the polymers will contribute to reducing the extreme soil losses in agriculture and forest land [79–82].

5. Conclusions

The effectiveness of PAM and PVA applied to different aggregate sizes showed different soil and water losses in the simulation experiments, with resistance to splash effect dependent on initial aggregate size. Moreover, total soil and water losses were different from the first and second rainfall simulation repetition. Our results showed that polymers did not importantly delay runoff generation in comparison to the control plot. However, both PAM and PVA reduced total runoff, sediment yield, and soil transported by splash considerably. For some reasons, such as the charge density and molecular weight, PAM could be more effective than PVA in reducing soil and water losses. In addition, sediment yield and water loss under the sequential rainfall were higher than during the first experiment. We hypothesize that it could be due to the fact that the drying time between the two experiments was not sufficient to reconnect the aggregates. Another factor could be the effect of the antecedent soil moisture, which was higher during the sequential rainfall too. The effectiveness of the polymers' application on soil aggregates increased when the size of the aggregates was also larger. Thus, we conclude that the application of polymer can be considered to be a more effective soil erosion control method when soil aggregates are larger than 6.4 mm, but further research must be done in order to understand other relevant aspects related to their economic and biophysical viability.

Conflicts of Interest: The authors declare no conflict of interest.

References

1. Schimel, D.S.; Braswell, B.H.; Holland, E.A.; McKeown, R.; Ojima, D.S.; Painter, T.H.; Parton, W.J.; Townsend, A.R. Climatic, edaphic, and biotic controls over storage and turnover of carbon in soils. Glob. Biogeochem. *Cycles* **2012**, *8*, 279–293. [CrossRef]

2. Smith, P.; Cotrufo, M.F.; Rumpel, C.; Paustian, K.; Kuikman, P.J.; Elliott, J.A.; McDowell, R.; Griffiths, R.I.; Asakawa, S.; Bustamante, M.; et al. Biogeochemical cycles and biodiversity as key drivers of ecosystem services provided by soils. *Soil* **2015**, *1*, 665–685. [CrossRef]

3. Alewell, C.; Egli, M.; Meusburger, K. An attempt to estimate tolerable soil erosion rates by matching soil formation with denudation in Alpine grasslands. *J. Soils Sediments* **2015**, *15*, 1383–1399. [CrossRef]

4. Nearing, M.A.; Xie, Y.; Liu, B.; Ye, Y. Natural and anthropogenic rates of soil erosion. *Intern. Soil Water Cons. Res.* **2017**, *5*, 77–84. [CrossRef]

5. Raich, J.W.; Potter, C.S. Global patterns of carbon dioxide emissions from soils. *Glob. Biogeochem. Cycles* **1995**, *9*, 23–36. [CrossRef]

6. Delgado-Baquerizo, M.; Maestre, F.T.; Gallardo, A.; Bowker, M.A.; Wallenstein, M.D.; Quero, J.L.; Ochoa, V.; Gozalo, B.; García-Gómez, M.; Soliveres, S.; et al. Decoupling of soil nutrient cycles as a function of aridity in global drylands. *Nature* **2013**, *502*, 672–676. [CrossRef]

7. Keesstra, S.; Mol, G.; de Leeuw, J.; Okx, J.; de Cleen, M.; Visser, S. Soil-related Sustainable Development Goals: Four concepts to make land degradation neutrality and restoration work. *Land* **2018**, *7*, 133. [CrossRef]

8. García-Ruiz, J.M.; Beguería, S.; Nadal-Romero, E.; González-Hidalgo, J.C.; Lana-Renault, N.; Sanjuána, Y. A meta-analysis of soil erosion rates across the world. *Geomorphology* **2015**, *239*, 160–173.

9. Ochoa, P.A.; Fries, A.; Mejía, D.; Burneo, J.I.; Ruíz-Sinoga, J.D.; Cerdà, A. Effects of climate, land cover and topography on soil erosion risk in a semiarid basin of the Andes. *Catena* **2016**, *140*, 31–42. [CrossRef]

10. Karydas, C.G.; Sekuloska, T.; Silleos, G.N. Quantification and site-specification of the support practice factor when mapping soil erosion risk associated with olive plantations in the Mediterranean island of Crete. *Environ. Monit. Assess.* **2009**, *149*, 19–28. [CrossRef]

11. Acín-Carrera, M.; José Marques, M.; Carral, P.; Álvarez, A.M.; López, C.; Martín-López, B.; González, J.A. Impacts of land-use intensity on soil organic carbon content, soil structure and water-holding capacity. *Soil Use Manag.* **2013**, *29*, 547–556. [CrossRef]

12. Beguería, S.; Angulo-Martínez, M.; Gaspar, L.; Navas, A. Detachment of soil organic carbon by rainfall splash: Experimental assessment on three agricultural soils of Spain. *Geoderma* **2015**, *245–246*, 21–30. [CrossRef]

13. Buczko, U.; Bens, O.; Hüttl, R.F. Tillage effects on hydraulic properties and macroporosity in silty and sandy soils. *Soil Sci. Soc. Am. J.* **2006**, *70*, 1998–2007. [CrossRef]

14. Reynolds, W.D.; Lewis, J.K. A drive point application of the Guelph Permeameter method for coarse-textured soils. *Geoderma* **2012**, *187–188*, 59–66. [CrossRef]

15. Fischer, C.; Roscher, C.; Jensen, B.; Eisenhauer, N.; Baade, J.; Attinger, S.; Scheu, S.; Weisser, W.W.; Schumacher, J.; Hildebrandt, A. How do earthworms, soil texture and plant composition affect infiltration along an experimental plant diversity gradient in grassland? *PLoS ONE* **2014**, *9*, e98987. [CrossRef]

16. Al-Shammary, A.A.G.; Kouzani, A.Z.; Kaynak, A.; Khoo, S.Y.; Norton, M.; Gates, W. Soil bulk density estimation methods: A review. *Pedosphere* **2018**, *28*, 581–596. [CrossRef]

17. Xiao, H.; Liu, G.; Liu, P.; Zheng, F.; Zhang, J.; Hu, F. Developing equations to explore relationships between aggregate stability and erodibility in Ultisols of subtropical China. *Catena* **2017**, *157*, 279–285. [CrossRef]

18. Barthès, B.; Roose, E. Aggregate stability as an indicator of soil susceptibility to runoff and erosion; validation at several levels. *Catena* **2002**, *47*, 133–149. [CrossRef]

19. Mamedov, A.I.; Huang, C.; Aliev, F.A.; Levy, G.J. Aggregate stability and water retention near saturation characteristics as affected by soil texture, aggregate size and polyacrylamide application. *Land Degrad. Dev.* **2017**, *28*, 543–552. [CrossRef]

20. Hartley, W.; Riby, P.; Waterson, J. Effects of three different biochars on aggregate stability, organic carbon mobility and micronutrient bioavailability. *J. Environ. Manag.* **2016**, *181*, 770–778. [CrossRef]

21. Martínez-Casasnovas, J.A.; Ramos, M.C.; García-Hernández, D. Effects of land-use changes in vegetation cover and sidewall erosion in a gully head of the Penedès region (northeast Spain). *Earth Surf. Proc. Land.* **2009**, *34*, 1927–1937. [CrossRef]

22. Smith, J.V.; Sullivan, L.A. Construction and maintenance of embankments using highly erodible soils in the Pilbara, North-Western Australia. *Intern. J. GEOMATE* **2014**, *6*, 897–902. [CrossRef]

23. Cerdà, A.; Rodrigo-Comino, J.; Giménez-Morera, A.; Novara, A.; Pulido, M.; Kapović-Solomun, M.; Keesstra, S.D. Policies can help to apply successful strategies to control soil and water losses. The case of chipped pruned branches (CPB) in Mediterranean citrus plantations. *Land Use Policy* **2018**, *75*, 734–745. [CrossRef]

24. Di Prima, S.; Marrosu, R.; Lassabatere, L.; Angulo-Jaramillo, R.; Pirastru, M. In situ characterization of preferential flow by combining plot- and point-scale infiltration experiments on a hillslope. *J. Hydrol.* **2018**, *563*, 633–642. [CrossRef]

25. Keesstra, S.D.; Rodrigo-Comino, J.; Novara, A.; Giménez-Morera, A.; Pulido, M.; Di Prima, S.; Cerdà, A. Straw mulch as a sustainable solution to decrease runoff and erosion in glyphosate-treated clementine plantations in Eastern Spain. An assessment using rainfall simulation experiments. *Catena* **2019**, *174*, 95–103. [CrossRef]

26. Novara, A.; Gristina, L.; Guaitoli, F.; Santoro, A.; Cerdà, A. Managing soil nitrate with cover crops and buffer strips in Sicilian vineyards. *Solid Earth* **2013**, *4*, 255–262. [CrossRef]

27. Davies, K.; Fullen, M.A.; Booth, C.A. A pilot project on the potential contribution of palm-mat geotextiles to soil conservation. Earth Surf. Process. *Landforms* **2006**, *31*, 561–569. [CrossRef]

28. Giménez-Morera, A.; Ruiz Sinoga, J.D.; Cerdà, A. The impact of cotton geotextiles on soil and water losses from Mediterranean rainfed agricultural land. *Land Degrad. Dev.* **2010**, *21*, 210–217. [CrossRef]

29. Pulido, M.; Schnabel, S.; Lavado Contador, J.F.; Lozano-Parra, J.; González, F. The Impact of Heavy Grazing on Soil Quality and Pasture Production in Rangelands of SW Spain. *Land Degrad. Dev.* **2018**, *29*, 219–230. [CrossRef]

30. Lasanta, T.; Nadal-Romero, E.; Arnáez, J. Managing abandoned farmland to control the impact of re-vegetation on the environment. The state of the art in Europe. *Environ. Sci. Policy* **2015**, *52*, 99–109. [CrossRef]

31. Ben-Salem, N.; Álvarez, S.; López-Vicente, M. Soil and water conservation in rainfed vineyards with common sainfoin and spontaneous vegetation under different ground conditions. *Water* **2018**, *10*, 1058. [CrossRef]

32. Hueso-González, P.; Martínez-Murillo, J.F.; Ruiz-Sinoga, J.D. Effects of topsoil treatments on afforestation in a dry Mediterranean climate (southern Spain). *Solid Earth* **2016**, *7*, 1479–1489. [CrossRef]

33. Cao, Y.; Wang, B.; Guo, H.; Xiao, H.; Wei, T. The effect of super absorbent polymers on soil and water conservation on the terraces of the loess plateau. *Ecol. Eng.* **2017**, *102*, 270–279. [CrossRef]

34. Blanco-Canqui, H.; Lal, R. *Principles of Soil Conservation and Management*; Springer Science + Business Media B.V.: Columbus, OH, USA, 2008. [CrossRef]

35. Gabriels, D. Application of soil conditioners for agriculture and engineering. In *Soil Colloids and Their Association in Aggregates*; De Boodt, M.F., Hayes, M., Herbillon, A., Eds.; Plenum Press: New York, NY, USA, 1990; pp. 557–565.

36. Sojka, R.E.; Lentz, R.D. Time for yet another look at soil conditioners. *Soil Sci.* **1994**, *158*, 233–234. [CrossRef]

37. Heitner, H.I. Flocculating agents. In *Encyclopedia of Chemical Technology*, 4th ed.; Kroschwitz, J.I., Howe-Grant, M., Eds.; John Wiley & Sons, Inc.: Hoboken, NJ, USA, 1994; Available online: https://doi.org/10.1002/0471238961 (accessed on 4 May 2019).

38. de Vleeschauwer, D.; Lal, R.; De Boodt, M. Comparison of detachability indices in relation to soil erodibility for some important Nigerian soils. *Pedologie* **1978**, *1*, 5–20.

39. Chiellini, E.; Corti, A.; Politi, B.; Solaro, R. Adsorption/desorption of polyvinyl alcohol on solid substrates and relevant biodegradation. *J. Polym. Environ.* **2000**, *8*, 67–79. [CrossRef]

40. Laird, D.A. Bonding between polyacrylamide and clay mineral surfaces. *Soil Sci.* **1997**, *162*, 826–832. [CrossRef]

41. Lu, J.H.; Wu, L.; Letey, J. Effects of soil and water properties on anionic polyacrylamide sorption. *Soil Sci. Soc. Am. J.* **2002**, *66*, 578–584. [CrossRef]

42. McLaughlin, R.A.; Bartholomew, N. Soil factors influencing suspended sediment flocculation by polyacrylamide. *Soil Sci. Soc. Am. J.* **2007**, *71*, 537–544. [CrossRef]

43. Kussainova, M.; Durmuş, M.; Erkoçak, A.; Kızılkaya, R. Soil dehydrogenase activity of natural macro aggregates in a toposequence of forest soil. *Eurasian J. Soil Sci.* **2013**, *2*, 69–75.

44. Bogunovic, I.; Bilandzija, D.; Andabaka, Z.; Stupic, D.; Rodrigo-Comino, J.; Cacic, M.; Brezinscak, L.; Maletic, E.; Pereira, P. Soil compaction under different management practices in a Croatian vineyard. *Arab. J. Geosci.* **2017**, *10*, 340. [CrossRef]

45. Bagagiolo, G.; Biddoccu, M.; Rabino, D.; Cavallo, E. Effects of rows arrangement, soil management, and rainfall characteristics on water and soil losses in Italian sloping vineyards. *Environ. Res.* **2018**, *166*, 690–704. [CrossRef] [PubMed]

46. Lieskovský, J.; Kenderessy, P. Modelling the effect of vegetation cover and different tillage practices on soil erosion in vineyards: A case study in Vráble (Slovakia) using WATEM/SEDEM. *Land Degrad. Dev.* **2014**, *25*, 288–296. [CrossRef]

47. Plante, A.F.; Feng, Y.; McGill, W.B. A modeling approach to quantifying soil macroaggregate dynamics. *Can. J. Soil Sci.* **2002**, *82*, 181–190. [CrossRef]

48. Marzen, M.; Iserloh, T.; Casper, M.C.; Ries, J.B. Quantification of particle detachment by rain splash and wind-driven rain splash. *Catena* **2015**, *127*, 135–141. [CrossRef]

49. Soil Survey Staff. *Keys to Soil Taxonomy*, 12th ed.; USDA-Natural Resources Conservation Service: Washington, DC, USA, 2014.

50. Turkish Republic General Directorate of Meteorology. 2017. Available online: https://www.mgm.gov.tr (accessed on 30 January 2018).

51. Wischmeier, W.H.; Smith, D.D. *Predicting Rainfall Erosion Losses: A Guide to Conservation Planning*; Agriculture Handbook No. 537; USDA/Science and Education Administration: Washington, DC, USA, 1978.

52. Eijkelkamp, Product Manual. 2015. Available online: https://www.eijkelkamp.com/download.php?file=M10906e_Rainfall_simulator_30f2.pdf. (accessed on 30 January 2018).

53. Christiansen, J.E. *Irrigation by Sprinkling*; California Agriculture Experiment Station Bulletin 670; University of California: Berkley, CA, USA, 1942.

54. Van Dijk, A.I.J.M.; Bruijnzeel, L.A.; Rosewell, C.J. Rainfall intensity-kinetic energy relationships: A critical literature appraisal. *J. Hydrol.* **2002**, *261*, 1–23. [CrossRef]

55. IBM Corp. USA. IBM SPSS Statistics 24 Brief Guide. Available online: http://public.dhe.ibm.com/software/analytics/spss/documentation/statistics/24.0/en/client/Manuals/IBM_SPSS_Statistics_Brief_Guide.pdf (accessed on 30 April 2019).

56. Chaplot, V.; Le Bissonnais, Y. Field measurements of interrill erosion under -different slopes and plot sizes. *Earth Surf. Process. Landf.* **2000**, *25*, 145–153. [CrossRef]

57. Sadeghi, S.H.R.; Seghaleh, M.B.; Rangavar, A.S. Plot sizes dependency of runoff and sediment yield estimates from a small watershed. *Catena* **2013**, *102*, 55–61. [CrossRef]

58. de Lima, J.L.M.P.; Singh, V.P. The influence of the pattern of moving rainstorms on overland flow. *Adv. Water Resour.* **2002**, *25*, 817–828. [CrossRef]

59. Sadeghi, S.H.; Kiani Harchegani, M.; Asadi, H. Variability of particle size distributions of upward/downward splashed materials in different rainfall intensities and slopes. *Geoderma* **2017**, *290*, 100–106. [CrossRef]

60. Taboada, M.A.; Barbosa, O.A.; Rodríguez, M.B.; Cosentino, D.J. Mechanisms of aggregation in a silty loam under different simulated management regimes. *Geoderma* **2004**, *123*, 233–244. [CrossRef]

61. Barry, P.V.; Stott, D.E.; Turco, R.F.; Bradford, J.M. Organic polymers' effect on soil shear strength and detachment by single raindrops. *Soil Sci. Soc. Am. J.* **1991**, *55*, 799–804. [CrossRef]

62. Nadler, A.; Perfect, E.; Kay, B.D. Effect of polyacrylamide application on the stability of dry and wet aggregates. *Soil Sci. Soc. Am. J.* **1996**, *60*, 555–561. [CrossRef]

63. Nishimura, T.; Yomamato, T.; Suzuki, S.; Kato, M. Effect of gypsum and polyacrylamide application on erodibility of an acid Kunigami Mahji Soil. *Soil Sci. Plant Nutr.* **2005**, *51*, 641–644. [CrossRef]

64. Mamedov, A.I.; Beckmann, S.; Huang, C.; Levy, G.J. Aggregate stability as affected by polyacrylamide molecular weight, soil texture, and water quality. *Soil Sci. Soc. Am. J.* **2007**, *71*, 1909–1918. [CrossRef]

65. Fernández-Raga, M.; Palencia, C.; Keesstra, S.; Jordán, A.; Fraile, R.; Angulo-Martínez, M.; Cerdà, A. Splash erosion: A review with unanswered questions. *Earth-Sci. Rev.* **2017**, *171*, 463–477. [CrossRef]

66. Tisdall, J.M.; Oades, J.M. Organic matter and water-stable aggregates in soils. *J. Soil Sci.* **1982**, *33*, 141–163. [CrossRef]

67. Singer, M.J.; Shainberg, I. Mineral soil surface crusts and wind and water erosion. *Earth Surf. Process. Landf.* **2004**, *29*, 1065–1075. [CrossRef]

68. Burguet, M.; Taguas, E.V.; Cerdà, A.; Gómez, J.A. Soil water repellency assessment in olive groves in Southern and Eastern Spain. *Catena* **2016**, *147*, 187–195. [CrossRef]

69. Ben-Hur, M.; Malik, M.; Letey, J.; Mingelgrin, U. Adsorption of polymers on clays as affected by clay charge and structure, polymer properties, and water quality. *Soil Sci.* **1992**, *153*, 349–356. [CrossRef]

70. Miller, W.P.; Willis, R.L.; Levy, G.J. Aggregate stabilization in kaolinitic soils by low rates of anionic polyacrylamide. *Soil Use Manag.* **1998**, *14*, 101–105. [CrossRef]

71. Asano, M.; Wagai, R. Evidence of aggregate hierarchy at micro- to submicron scales in an allophanic Andisol. *Geoderma* **2014**, *216*, 62–74. [CrossRef]

72. Oades, J.M. Soil organic matter and structural stability: Mechanism and implications for management. *Plant Soil* **1984**, *76*, 319–337. [CrossRef]

73. Kay, B.D. Rates of change of soil structure under different systems. *Adv. Soil Sci.* **1990**, *12*, 1–52.

74. Levy, G.J.; Miller, W.P. Polyacrylamide adsorption and aggregate stability. *Soil Till. Res.* **1999**, *51*, 121–128. [CrossRef]

75. Parlak, M. Study on splash erosion with interaction of different kinetic energy flux and soil texture. *J. Agric. Sci.* **2009**, *15*, 341–347.

76. Leguedois, S.; Le Bissonnais, Y. Size fractions resulting from an aggregate stability test, interrill detachment and transport. *Earth Surf. Proc. Land.* **2004**, *29*, 1117–1129. [CrossRef]

77. Gumiere, S.J.; Le Bissonnais, Y.; Raclot, D. Soil resistance to interill erosion: Model parameterization and sensitivity. *Catena* **2009**, *77*, 274–284. [CrossRef]

78. Rodrigo-Comino, J.; Giménez-Morera, A.; Panagos, P.; Pourghasemi, H.R.; Pulido, M.; Cerdà, A. The potential of straw mulch as a nature-based solution in olive groves treated with glyphosate. A biophysical and socio-economic assessment. *Land Degrad. Dev.* **2019**, in press. [CrossRef]

79. Salesa, D.; Terol, E.; Cerdà, A. Soil erosion on the "El Portalet" mountain trails in the Eastern Iberian Peninsula. *Sci. Total Environ.* **2019**, *661*, 504–513. [CrossRef] [PubMed]

80. Wenger, A.S.; Atkinson, S.; Santini, T.; Falinski, K.; Hutley, N.; Albert, S.; Horning, N.; Watson, J.E.M.; Mumby, P.J.; Jupiter, S.D. Predicting the impact of logging activities on soil erosion and water quality in steep, forested tropical islands. *Environ. Res. Lett.* **2018**, *13*, 044035. [CrossRef]

81. Plastina, A.; Liu, F.; Miguez, F.; Carlson, S. Cover crops use in Midwestern US agriculture: Perceived benefits and net returns. *Renew. Agric. Food Syst.* **2018**, 1–11. [CrossRef]

82. Ghosh, B.N.; Dogra, P.; Sharma, N.K.; Bhattacharyya, R.; Mishra, P.K. Conservation agriculture impact for soil conservation in maize–wheat cropping system in the Indian sub-Himalayas. *Intern. Soil Water Conserv. Res.* **2015**, *3*, 112–118. [CrossRef]